Evolution of disclinations in cholesteric liquid crystals

F. Zhang and D.-K. Yang*
Chemical Physics Program, Liquid Crystal Institute, Kent State University, Kent, Ohio 44242
(Received 10 January 2002; revised manuscript received 12 July 2002; published 4 October 2002)

We studied the evolution of defect lines (oily streaks) in cholesteric liquid crystals. In contrast to nematic liquid crystals, there were no interactions between the defect lines in cholesteric liquid crystals. We observed experimentally that individual open defect segments shrank with time with a linear relation, and individual defect loops shrank with time with a square root relation. We also observed that the defects in cholesteric liquid crystals were mainly interconnected loops, and the total length of the defect lines decreased with time logarithmically because of the distribution of loop size. The decay constant depended on the helical pitch of the liquid crystal and temperature.

DOI: 10.1103/PhysRevE.66.041701 PACS number(s): 61.30.Jf, 47.53.+n, 05.70.Fh

INTRODUCTION

The evolution of defects in physical systems is of considerable interest [1–4]. The dynamic behavior of the defects is expected to be dependent on the dimensionality, symmetry, and interaction between defects of the system. Liquid crystalline phases possess various symmetries in one, two, and three dimensions. They are very useful systems to be used to study the dynamics of defects, because of their low experimental cost, the time scale involved, and ease of experimental observation [5–8]. Considerable work has been done on the dynamic behavior of defects in nematic liquid crystals which consist of elongated organic molecules [5–9]. They possess long range orientational order but not positional order. There are interactions between line defects (disclinations) in nematic liquid crystals. The dynamics of the coarsening of the line defects is governed by $\rho \propto t^{-1}$, where ρ is the density of the defect lines [5,6].

Cholesteric liquid crystals are similar locally to nematic liquid crystals: the average direction of the long axis of the molecules is along a common direction called the director. The director, however, twists around a perpendicular axis [9]. When the pitch of the helical structure is short, the cholesteric phase can be considered an incompressible layered mesophase. The most common defects in cholesteric liquid crystals are oily streaks [10,11]. The defects are localized because the director distortion occurs within a small region with size comparable to the cell thickness. There is no interaction between the defect lines. Zapotocky *et al.* studied the coarsening of the line defects (oily streaks) in cholesteric liquid crystals [12]. They observed that in a pure cholesteric liquid crystal system the defect density ρ has the temporal dependence of $(1-t/t_{\mathrm{dec}})$. Studying the defects in cholesteric liquid crystals is also of practical importance. In many cholesteric applications, such as cholesteric polarizers and light shutters [13–15], perfect planar texture without defects is desired. Understanding the defects can help to eliminate them.

We used two methods to experimentally study the dynamics of the oily streaks in cholesteric liquid crystals. In the first method, we used an optical microscope to examine the evolution of the defect lines. In the second method, we monitored the capacitance of the cholesteric cells as a function of time. The capacitance which is sensitive to the density of the defect lines where some molecules are perpendicular to the cell surface, instead of being parallel to the cell surface as in the planar texture. We observed that the density of the defect lines decreased logarithmically with time. Based on the assumption that there is a distribution of the lengths of the defect lines, we also developed a model which can explain the observed dynamic behavior of the defect lines.

EXPERIMENT

The cholesteric liquid crystal was a mixture of nematic liquid crystal BL006 and chiral dopant CE1 (from Merck). The pitch of the liquid crystal was adjusted by varying the concentration of CE1. The mixture was filled in a vacuum chamber into cells consisting of two parallel glass plates with transparent ITO electrodes. The cell thickness h was 5 μm. The inner surface of the cell was coated with polyimide and rubbed to generate homogeneous alignment of the liquid crystal. This liquid crystal has a positive dielectric anisotropy and tends to align parallel to an externally applied electric field. At zero field, the liquid crystal was in the planar texture with the helical axis perpendicular to the cell surface. When a sufficiently high field was applied across the cell, the liquid crystal was switched to the homeotropic texture where the liquid crystal director was aligned parallel to the field. The applied field was then reduced slowly (in a few seconds) to zero; the liquid crystal was transformed into the focal conic texture and then into the planar texture. There were many defect lines, called ''oily streaks,'' where the cholesteric layers were bent. The oily streaks were not favored by the alignment layer and had a higher free energy. They shrank and eventually disappeared.

We used an optical microscope with crossed polarizers to study the evolution of the defect lines. Figure 1 shows the microphotographs taken during the evolution. They were taken at 0, 10, 60, and 460 s, respectively, after the applied field was removed. The pitch of the sample was 1.07 μm. The defects were mainly interconnected loops. There were more small loops. The defects shrank with time. Smaller

*Corresponding author. Email address: dyang@lci.kent.edu

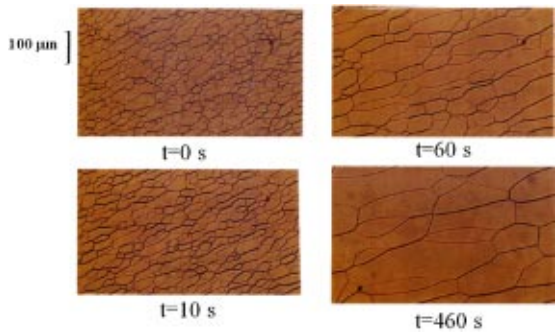

FIG. 1. Microphotographs of the defects in the cholesteric cell taken in the evolution.

loops disappeared earlier. There was also a distribution in the lateral size of the defect lines. Smaller lateral size defect lines annihilated faster than larger lateral size defect lines. Because of impurities and surface irregularities in the sample, there were some residual defects even after a long evolution time [12]. The defect loops were elongated in the rubbing direction of the alignment layers.

At later stages of the annihilation, using a video camera, we were able to photograph some isolated defects. Figure 2 shows the shrinking of a defect line. The time interval between two consecutive photographs was 0.5 ms. The length of the defect as a function of time is plotted in Fig. 3. Approximately, the length of the defect decreased linearly with time at the rate of 190 μm/ms. Figure 4 shows the shrinking of a defect loop with time. The time interval between two consecutive photographs was 2 s. At the beginning the loop was an ellipse. It gradually changed into a circle because of the positive line tension. The circumference l was approximately calculated by $l=\pi(a+b)$, where a and b were the lengths of the major and minor axes, respectively. l as a function of time is plotted in Fig. 5. The shrinking rate of the loop was much slower than that of the linear defect. We discuss the shrinking rate more below. When the radius of the defect loop became close to the lateral size of the defect, the situation was very complicated and will not be discussed in this paper.

We had a difficult time measuring the total length of the defects as a function of time by using image analysis. Only a small portion of the sample was observed under the optical microscope. We found that the temporal behavior of the total length of the defect was similar to that of the capacitance of the cell, which will be discussed below, but the error bar of

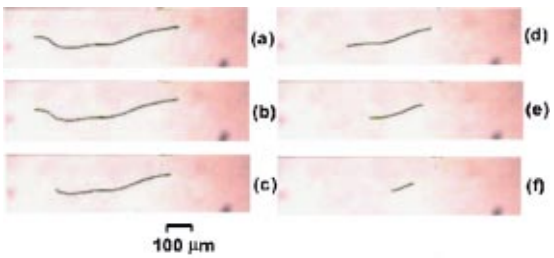

FIG. 2. Microphotographs showing the shrinking of the open defect line.

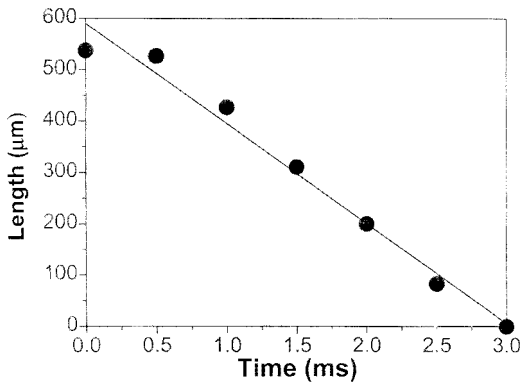

FIG. 3. The length of the open defect line vs time. Symbols, experimental data; solid line, the linear fit.

the total length of the defects was large. We used another technique, dielectric method, to study the evolution of the defect lines, where the capacitance of the sample was monitored as a function of time. The voltage used in the experiment was sinusoidal wave with an amplitude of 100 mV and a frequency of 1 kHz. When the liquid crystal was in the planar texture, the liquid crystal director was parallel to the cell surface, and the capacitance per unit area was $\varepsilon_0\varepsilon_\perp/h$. When the liquid crystal director was perpendicular to the cell surface, the capacitance was $\varepsilon_0\varepsilon_\parallel/h$, which was larger than $\varepsilon_0\varepsilon_\perp/h$. In the oily streaks, the liquid crystal director was tilted away from the plane of the cell. The tilt angle from the cell surface of the liquid crystal director changed gradually from 90° to 0° from the middle plane of the defect to the cell surface. Thus a higher capacitance than the planar texture was produced. The orientation of the liquid crystal in the defect line was independent of the density of the defect lines as long as the distance between the defect lines was more than a few h. Thus the increment of capacitance produced by per unit length defect was a constant. As an approximation, the capacitance C of the cell was linearly proportional to the total length L of the defect lines.

$$C=C_0+C_1L, \tag{1}$$

where C_0 was the capacitance of the planar texture and C_1 was a constant dependent on the lateral size of the defect line. Figure 6 shows the capacitance of a cell at various

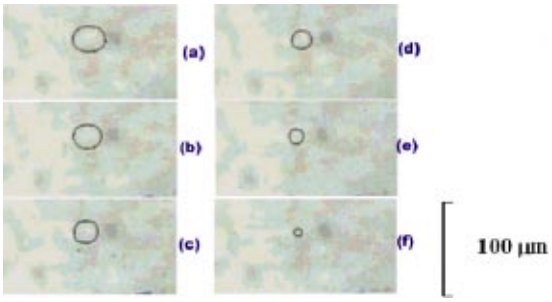

FIG. 4. Microphotographs showing the shrinking of the closed defect loop.

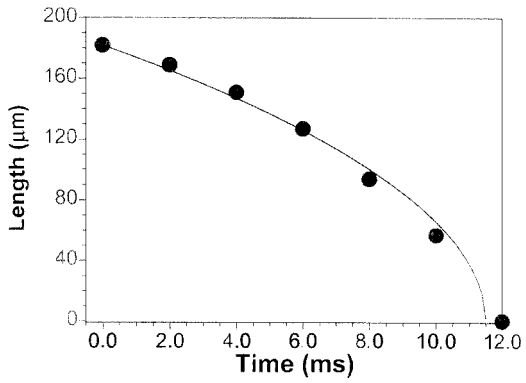

FIG. 5. The length of the closed defect loop vs time. Symbols, experimental data; solid line, the square root fit.

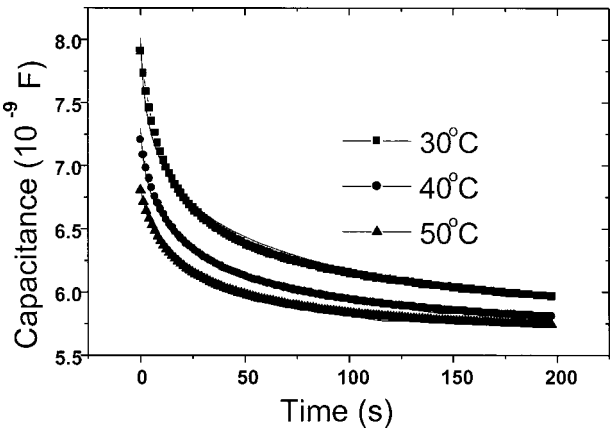

FIG. 6. The capacitance of the cholesteric cell as a function of time at various temperatures.

temperatures as a function of time. The pitch of the cell was 0.53 μm. The curves were fitted well by logarithmic functions.

ANALYSIS

Let us first consider the dynamics of individual defect lines. A cholesteric liquid crystal with a short pitch can be regarded as an incompressible layered material with layer thickness equal to half pitch. The defects under study in this paper are oily streaks where the layers are bent. The bending of the layers only occurs in a region with linear size comparable to the cell thickness, and the lateral sizes of the defects are also comparable to the cell thickness. Therefore there is no interaction between two defect lines unless the distance between them becomes comparable to the cell thickness. Consider a defect line; its total free energy (elastic energy) F is related to its length l by

$$F = fl, \tag{2}$$

independent of whether the defect line is a closed loop (when the radius is much larger than the lateral size of the defect) or an open segment, where f is the free energy per unit length. Note the lateral sizes of the defect lines may be different and the free energy densities are different. Because the defects cost energy, they are not stable and therefore shrink with time. Dynamics involved in liquid crystal is usually overdamped, i.e., the elastic force is balanced by the viscosity force. For an open linear defect line, the decrease of the length of the defect line is described by

$$\gamma_1 \frac{\partial l}{\partial t} = -\frac{\partial F}{\partial l} = -f, \tag{3}$$

where γ_1 is the effective viscosity coefficient. Equation (3) gives

$$l = l_0 - \frac{f}{\gamma_1} t \quad \text{for } t \leqslant t_1 = \frac{l_0}{f/\gamma_1}, \tag{4}$$

where l_0 is the initial length of the defect line. This linear behavior agrees with the experimental result shown in Fig. 3.

Because the defect shrinks from both ends, the real shrinking rate is $2f/\gamma_1$. By fitting the data, the shrinking rate $2f/\gamma_1$ is found to be 190 μm/s.

Here the defects are oily streaks whose free energy f is contributed by the bend elastic energy, defect core energy, anchoring energy at the cell surface, and the wall energy [11]. To estimate the order of magnitude of the free energy, we calculated the bend elastic energy. one. In the Lubensky–de Gennes coarse-grain theory [9], the bend elastic energy per unit length is given by

$$f = \int_P^h \frac{1}{2}\left(\frac{3}{8}K_{33}\right)\left(\frac{1}{r}\right)^2 r\,dr = \frac{3}{16}K_{33}\ln\left(\frac{h}{P}\right), \tag{5}$$

where K_{33} is the bend elastic constant. We do not know the value of K_{33} of the liquid crystal used in the experiment. In order to estimate the value of the viscosity coefficient γ_1, we use $K_{33}=10^{-11}$ N, $P=1.07$ μm, and $h=5$ μm. We get $f=2.8\times10^{-12}$ N. Then from the shrinking rate of the open linear defect we get $\gamma_1=3\times10^{-9}$ N s/m. We do not know how γ_1 is related to the rotational viscosity coefficient γ of the liquid crystal, which is usually on the order of 10^{-1} N s/m^2. Because of their dimensions γ_1 should equal the production of γ and a characteristic length which may be the linear molecular size.

For a circular defect loop with radius r which is much larger than the lateral size of the defect, the elastic energy caused by the curvature of the loop is negligible and the total elastic energy of the defect loop is $2\pi rf$, and the viscosity force is given by $-\gamma_2(2\pi r)(\partial r/\partial t)$. The dynamic equation is

$$\gamma_2(2\pi r)\frac{\partial r}{\partial t} = -\frac{\partial F}{\partial r} = -\frac{\partial(2\pi r f)}{\partial r} = -2\pi f, \tag{6}$$

where γ_2 is the effective viscosity coefficient of per unit length defect (note, γ_2 has a different unit from γ_1). Equation (6) gives

$$r = \sqrt{r_0^2 - \frac{2f}{\gamma_2}t} \quad \text{for } t \leqslant t_2 = \frac{r_0^2}{2f/\gamma_2}, \tag{7}$$

where r_0 is the initial radius of the defect loop. The circumference l of the loop as a function of time is

$$l=\sqrt{l_0^2-\frac{8\pi^2 f}{\gamma_2}t} \quad \text{for } t\leqslant t_2=\frac{l_0^2}{8\pi^2 f/\gamma_2}, \tag{8}$$

where l_0 is the initial circumference. Equation (8) fits fairly well the experimental data as shown in Fig. 5. By fitting the data, $8\pi^2 f/\gamma_2$ is found to be 2280 μm^2/s. Using the free energy calculated earlier, we get $\gamma_2=1\times10^{-1}$ N s/m^2. Although γ_2 is close to the rotational viscosity coefficient γ, we also do not know how they are related to each other. The shrinking rate of the defect loop is much slower than that of the open linear defect line. This is because of the different shrinking mechanisms involved. For the open linear defect line, only the molecules at the ends need to rotate to generate the shrinking. For the defect loop, all the molecules in the loop need to rotate to generate the shrinking.

Now we consider the total length of the defects in the sample. The defects are mainly loops interconnected at nodes. The circumferences of the loop are not the same but widely distributed. There are more smaller loops than larger loops. They all shrink with time. Smaller loops annihilate at earlier times. We attempted to derive an analytic expression for the total length of the defects, but did not succeed because of a lack of the distribution function of the defect loop size.

The experimental data of capacitance as a function data can be fitted best by a logarithmic function,

$$C=C_{\text{initial}}-C'\ln(\alpha t+1)$$
$$\text{for } t\leqslant\frac{1}{\alpha}[e^{(C_{\text{initial}}-C_{\text{stable}})/C'}-1], \tag{9}$$

where C_{initial} is the initial capacitance, C_{stable} is the stable capacitance at a time long after the field is removed, C' is the increment capacitance produced by the defects which will annihilate, and α is the decay constant. From Eq. (6), α is expected to be proportional to f/γ_2. The temperature dependence of the viscosity coefficient is described by $e^{\Delta E/k_BT}$ where ΔE is the energy barrier. The elastic energy f is approximately proportional to the pitch P [10], and therefore the decay constant is given by

$$\alpha=\alpha_0 P e^{-\Delta E/k_BT}, \tag{10}$$

where α_0 is a constant.

The capacitance vs time is shown in Fig. 6. The experimental data are represented by the symbols and the fitting by Eq. (10) is represented by the solid lines. The initial capacitance C_{initial} and the capacitance C_{stable} at a time long after the field was turned off were experimentally measured. The fitting parameters were C' and α. They were manually adjusted to obtain the minimum χ^2 error. The fitting was fairly good.

At different temperatures, the dielectric constants of the liquid crystal were different, and therefore different C' had to be used. The viscosity coefficient changed with temperature, and therefore the decay constant α was different at different temperatures. At higher temperature, the viscosity was lower, and therefore the defects annihilated faster. According to Eq. (10), $\ln\alpha\propto-\Delta E/k_BT$. The values of α at various temperatures for cells with various pitches are plotted in Fig. 7. $\ln\alpha$ vs $1/T$ was fitted considerably well by straight lines. For example, when the pitch was 0.53 μm, the energy barrier ΔE for the viscosity was 0.17 eV.

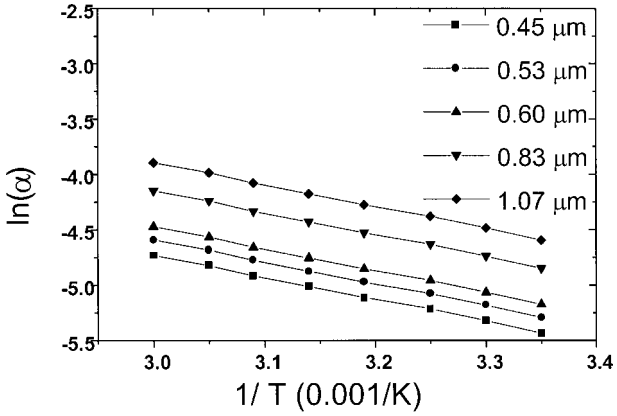

FIG. 7. The decay constant of cholesteric cells with various pitches vs inverse temperature.

The evolution of the defects in cholesteric liquid crystals was also pitch-dependent. The elastic energy per unit length of the defect line (oily streak) was linearly proportional to the helical pitch P [10]. The higher the elastic energy density, the higher the line tension of the defect line, and therefore the faster it shrank. The decay constant α obtained by fitting the experimental data as a function of P is shown in Fig. 8. A linear relation given by Eq. (10) described well the relation between α and P.

CONCLUSION

We studied the evolution of defects (oily streak) in cholesteric liquid crystals using optical microscopy. We observed that the shrinking of an individual open defect with time was governed by a linear relation, and the shrinking of a closed defect loop with time was governed by a square root relation. We also developed a technique to study the evolution of defects in cholesteric liquid crystals, in which the

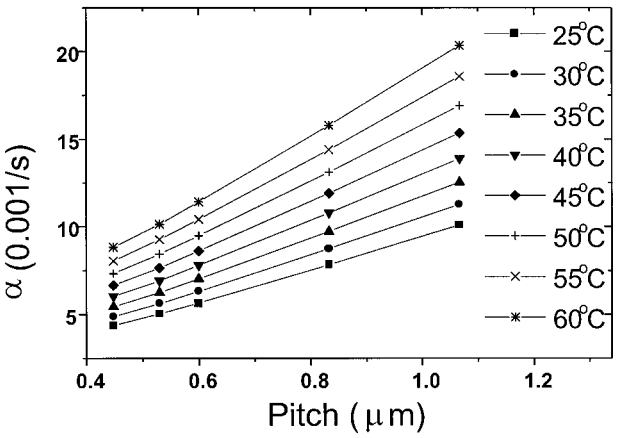

FIG. 8. The decay constant vs pitch at various temperatures.

capacitance of the liquid crystal cells was monitored as a function of time. We observed that the capacitance produced by the defects decreased logarithmically with time. Under the assumption that the total length of the defect lines in the ch cell was linearly related to the capacitance of the cell, the total length of the defects decreased logarithmically with time. This logarithmic temporal behavior was produced by a statistical effect that there was a distribution in the defect loop size when they were created. We have also studied the evolution of the defects at various temperatures and in samples with various pitches. The results are of importance in understanding evolution of defects in liquid crystal in general and useful in eliminating defects in cholesteric devices.

ACKNOWLEDGMENTS

This research was partially supported by the NSF under ALCOM Grant No. DMR89-20147. We also thank Professor P. Palffy-Muhoray, J. R. Kelly, and E. C. Gartland for stimulating discussions.

[1] H. Furukawa, Adv. Phys. **34**, 703 (1985).
[2] P. C. Hohenberg and B. I. Halperin, Rev. Mod. Phys. **49**, 435 (1977).
[3] P. W. Voorhees, J. Stat. Phys. **38**, 231 (1985).
[4] J. D. Gunton, M. San Miguel, and P. S. Sahni, in *Phase Transition and Critical Phenomena*, edited by C. Domb and J. L. Lebowwitz (Academic, London, 1983), p. 267.
[5] I. Chuang, N. Turok, and B. Yurke, Phys. Rev. Lett. **66**, 2472 (1991).
[6] I. Chuang, R. Durrer, N. Turok, and B. Yurke, Science **251**, 1336 (1991).
[7] I. Chuang, B. Yurke, A. Pargellis, and N. Turok, Phys. Rev. E **47**, 3343 (1993).
[8] A. Pargellis, P. Finn, J. W. Goodby, P. Yurke, and P. E. Cladis, Phys. Rev. E **46**, 7765 (1993).
[9] For a review on liquid crystals, see P. G. de Gennes and J. Prost, *The Physics of Liquid Crystals* (Oxford University Press, New York, 1993).
[10] S. Chandrasekhar, *Liquid Crystals*, 2nd ed. (Cambridge University Press, New York, 1997).
[11] O. D. Lavrentovich and D.-K. Yang, Phys. Rev. E **57**, R6269 (1998).
[12] M. Zapotocky, L. Ramos, P. Poulin, T. C. Lubensky, and D. A. Weitz, Science **283**, 209 (1999).
[13] D. J. Broer, J. A. M. M. van Haaren, G. N. Mol, and F. Leenhouts, Proc. Asia Display '95 , 735 (1995).
[14] L. Li and S. M. Faris, SID Intl. Symp. Digest Tech. Papers **27**, 111 (1996).
[15] M. Xu and D.-K. Yang, Appl. Phys. Lett. **70**, 720 (1997).